# Angular-dependent muon-spin rotation and torque magnetometry on the mixed state of the high-temperature superconductor $YBa_2Cu_3O_{7-\delta}$

C. Ager, F. Y. Ogrin, and S. L. Lee
*School of Physics and Astronomy, University of St. Andrews, St. Andrews, Fife KY16 9SS, United Kingdom*

C. M. Aegerter, S. Romer, H. Keller, and I. M. Savić
*Physik-Institut der Universität Zürich, CH-8057 Zürich, Switzerland*

S. H. Lloyd, S. J. Johnson, E. M. Forgan, T. Riseman, and P. G. Kealey
*School of Physics and Space Research, University of Birmingham, Birmingham B15 2TT, United Kingdom*

S. Tajima and A. Rykov
*Superconductivity Research Laboratory, ISTEC, Tokyo 135, Japan*
(Received 22 October 1999)

Muon-spin rotation ($\mu$SR) and torque magnetometry have been used to probe the anisotropy of an untwinned single crystal of $YBa_2Cu_3O_{7-\delta}$. The absence of twin planes allows the ratios of all three principal components of the superconducting effective mass tensor to be determined. The values for the in-plane anisotropy are in good agreement with values obtained by other techniques. The out-of-plane anisotropies as measured by $\mu$SR are also found to be in good agreement with other microscopic measurements, but somewhat lower than those resulting from torque measurements on this and other crystals.

## I. INTRODUCTION

A key feature of the high $T_c$ superconductors (HTSC's) that governs the structure of the flux lattice is the superconducting anisotropy.[1] This anisotropy is reflected in the ability of the superconducting charge carriers to screen magnetic fields, and is normally quantified as $\gamma=\lambda_c/\lambda_{ab}$, where $\lambda_c$ and $\lambda_{ab}$ are the penetration depths for currents flowing perpendicular and parallel to the superconducting copper oxide planes, respectively. In such anisotropic systems any anisotropy within the basal plane, between the *a* and *b* directions is often ignored. For a tetragonal system such as $Bi_{2.15}Sr_{1.85}CaCu_2O_{8+\delta}$ with $\gamma\sim 150$, such a uniaxial view is quite valid,[2] but for the orthorhombic system $YBa_2Cu_3O_{7+\delta}$ (YBCO) this uniaxial picture masks the subtle in-plane anisotropy, which may have important consequences for the structure of the vortex lattice in this compound. In general the most important element in the HTSC is the two-dimensional copper oxide planes, but the unit cell of YBCO contains several other key structural elements, including the one-dimensional copper oxide chains in YBCO and the double chain structure in the related compound $YBa_2Cu_4O_8$. These chains, which lie along the crystallographic *b* direction and act as charge reservoirs, could contribute to the superconducting condensate[3,4] and thus give rise to a measurable effect on the basal plane anisotropy. Determining the magnitude of this *ab* anisotropy can be particularly difficult in twinned crystals of YBCO, as the occurrence of planar defects (twin planes) parallel to the *c* direction cause the *a* and *b* directions in different parts of the crystal to coincide. Small flux grown crystals of YBCO, oxygenated to optimum doping, can be detwinned by applying uniaxial stress along the *a* direction ($b>a$) at moderately high temperatures, while the sample remains in the orthorhombic phase and loses little oxygen. One disadvantage of measuring with these crystals is their small size. Another technique has proved successful in the production of large untwinned crystals,[5] whereby uniaxial stress is applied, as before, and the crystals are heated under low oxygen pressure to above the orthorhombic-tetragonal phase transition. On cooling under the continued application of uniaxial stress the sample forms one orientation of the orthorhombic structure. Here we investigate the basal-plane anisotropy of a large untwinned crystal prepared in this way at SRL-ISTEC. This crystal is of such an appreciable extent ($\sim$0.5 cm$^3$) that it is ideal for a muon-spin rotation ($\mu$SR) investigation, where a determination of the three principal values of the penetration depth may be achieved. The sample was annealed in flowing oxygen at 490 °C, after which magnetization measurements showed the crystal to undergo a sharp transition to the superconducting state at $T_c=93.5$ K. In addition to the $\mu$SR measurements we have also constructed a phosphor bronze cantilever that has enabled us to carry out torque magnetometry measurements on the same single crystal, in order to compare the anisotropy measured by two different techniques.

## II. EXPERIMENT

### A. Muon spin rotation ($\mu$SR)

Time differential transverse field $\mu$SR experiments were carried out with low-momentum surface muons (29 MeV), produced with their spin antiparallel to their momentum, at the MUSR spectrometer at ISIS, UK, and on the $\pi$M3 beamline at PSI, Zurich. In transverse $\mu$SR muons come to rest in the sample and precess at a rate determined by the local internal field. In a type II superconductor this internal magnetic field arises from a regular array of vortices, each of which carries one quantum of magnetic flux $\phi=h/2e$, where *h* is Planck's constant and *e* is the charge of an electron. This

 

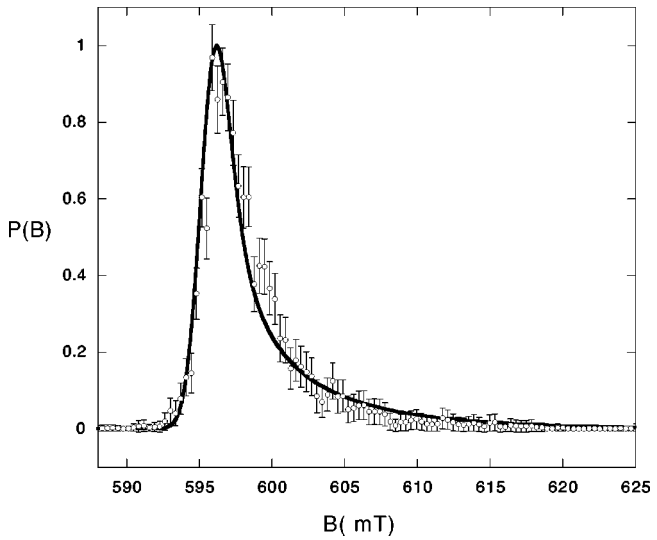


FIG. 1. Example of the field probability distribution for the field applied at $\theta=0°$ to the $c$ axis in the $ac$ plane. These data where taken at 10 K after cooling in an applied field of 600 mT on the $\pi$M3 beamline (PSI). The line shape is highly characteristic of the intrinsic structure of the flux vortex lattice: the cutoff at low fields corresponds to the minimum in the field distribution between flux lines; the peak corresponds to the most probable field value at the saddle point on a line connecting two flux lines; the long tail corresponds to the high field values close to the flux-line cores (see Ref. 6). The solid line is a simulation in the London limit of the field probability distribution for an ideal vortex lattice with an effective penetration depth $\lambda_{ab}=(\lambda_a\lambda_b)^{1/2}=150(10)$ nm. The uncertainty is the accuracy with which $\lambda_{ab}$ can be determined from the data assuming this model.

spatial modulation of the local flux density $B(r)$ is sampled by muons which are implanted randomly over the flux lattice. By Fourier transform (FT) of the positron spectrum formed on decay of the muons, one may obtain the $\mu$SR line shape, or frequency distribution.[6] This frequency distribution is an excellent measure of the probability distribution $p(B)$ of the internal field values of the superconductor and thus is intimately related to the spatial distribution $B(r)$. In this way the $\mu$SR line shape may be used to yield important structural information concerning the flux lattice.[7–10] Extraction of this probability distribution from the positron decay spectrum is seen to involve a FT. Conventional fast FT may be employed, but in order to suppress noise due to Poisson counting statistics and produce cleaner line shapes for quantitative analysis we have utilized a maximum entropy technique.[11,12] A typical line shape is shown in Fig. 1. This technique is particularly useful if one wants to perform a systematic study of the moments of $p(B)$, which can be extremely sensitive to the presence of noise. The details of this method are outlined in Refs. 11, 13, and 12. On the $\pi$M3 beamline the field is applied parallel to the momentum of the incident muons, which are spin rotated to allow this setup to conform to a transverse field geometry. On the MUSR beamline the muons are not spin rotated and the field is applied perpendicular to the incident beam. The setup of the MUSR spectrometer allows the field to be applied at small angles to the superconducting planes with a large cross-sectional area of the sample presented to the beam. The converse is true for $\pi$M3 where decreasing the angle between the field and the

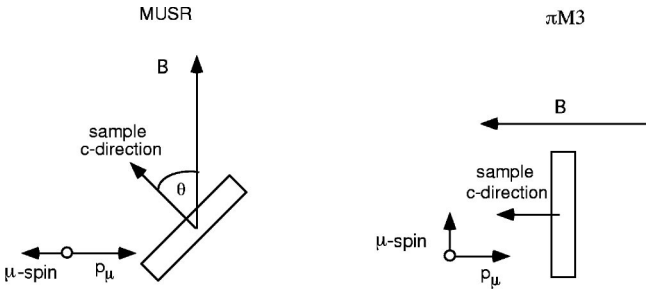


FIG. 2. A plan view of the experimental geometry at the MUSR spectrometer (ISIS) and at the spectrometer on the $\pi$M3 beamline (PSI). Transverse $\mu$SR requires the muon spin to have a component perpendicular to the field. For MUSR it can be seen that the plate-like crystal shape, coupled with the longitudinal spin polarization of the beam, favors larger angles $\theta$ between the field and the crystallographic $c$ direction, so that a larger cross section of the sample is presented to the beam. MUSR is thus ideal for measuring with angles of $c$ to the applied field of $45°<\theta\leqslant 90°$, while conversely the transverse polarization of the $\pi$M3 beam is ideal for covering the range $0°\leqslant\theta<45°$.

planes decreases the cross-sectional area presented to the beam (see Fig. 2). As a consequence of these factors the above facilities offer very different but complementary geometries for the angular investigation of HTSC. Special attention was paid in our experiments to ensure that the same experimental setup was followed on both spectrometers for all orientations of the crystal. In particular, all the muons not stopping in the sample were stopped in a haematite sample holder. The rapid depolarization at very early times of these muons landing outside the sample prevents them from contributing significantly to the oscillating component of the measured signal, which then reflects only the influence of the sample on the muon precession.[6]

A measure of the width of the field distribution is given by the square root of the second moment of the $\mu$SR line shape. In London theory this is related to the penetration depth via[6]

$$\langle \Delta B^2\rangle^{1/2}(T)=\left(\sum_{q\neq 0}\frac{\langle B\rangle^2}{(\mathbf{1}+\lambda(T)^2q^2)^2}\right)^{1/2}. \tag{1}$$

Here $q$ is a reciprocal lattice vector and $\lambda(T)$ is the penetration depth in a plane perpendicular to the field direction. In general, for orthorhombic symmetry we may describe the superconducting anisotropy by a normalized effective mass tensor[14]

$$\mathcal{M}_{\rm eff}=\begin{pmatrix} m_1 & 0 & 0\\ 0 & m_2 & 0\\ 0 & 0 & m_3\end{pmatrix},$$

where $m_i=M_i/M_{\rm av}$, $M_{\rm av}=(M_1M_2M_3)^{1/3}$, and $M_i$ is the effective mass of an electron flowing along the $i$th principal axis. The effective penetration depth for fields directed along the $i$th principal axes of the effective mass tensor is then given by

$$\lambda_{\rm eff}^2=\lambda_j\lambda_k\propto\sqrt{\frac{1}{M_jM_k}}. \tag{2}$$

Thiemann and co-workers[14] have calculated the Fourier components of the internal field distribution of a well ordered flux line lattice for rotation of the applied field about one of the principal axes. By extending their analysis it was subsequently shown that the angular variation of the second moment of the internal field distribution is given by[15–18]

$$\langle \Delta B^2 \rangle^{1/2}(T)(\theta) = \langle \Delta B^2 \rangle^{1/2}(0)(\cos^2\theta + 1/\gamma_{ij}^2 \sin^2\theta)^{1/2}, \tag{3}$$

where $\gamma_{ij} = \sqrt{M_j/M_i} = \lambda_i/\lambda_j$, and $\theta$ is the angle between the applied field and the $i$th axis, for rotations about the $k$th axis. In previous experiments on *twinned* YBCO crystals, Eq. (3) was found to be a good description of the angular dependence of the muon depolarization rate.[15,16,19] In the present work, by performing measurements as a function of angle about two of the three principal directions of the effective mass tensor, we have characterized the anisotropy of an untwinned crystal of YBCO.

For all measurements the sample was first cooled to 10 K in the presence of the applied field. Figure 1 shows an example of the probability distribution of internal fields $p(B)$ for the geometry with the field parallel to the $c$ direction. Small angle neutron scattering (SANS) measurements have already been performed on the *same* crystal, which reveal that the lattice has approximately triangular symmetry with distortions due to the in-plane anisotropy.[20] In that work, for the geometry with the field parallel to the $c$ direction, an estimate of the effective in-plane penetration depth $\lambda_{ab} = (\lambda_a \lambda_b)^{1/2}$ yielded $\lambda_{ab} = 138(5)$ nm. The most reliable method to obtain the penetration depth from the $\mu$SR line shape is to fit the data to a model, which in principle should be a distorted triangular lattice of vortex lines. For the geometry with the field directed along any principal axis of the effective mass tensor, a suitable scaling shows that probability distribution $p(B)$ reduces to that of anisotropic superconductor with an effective penetration depth which in this case is[17] $\lambda_{ab} = (\lambda_a \lambda_b)^{1/2}$. This result is in accord with numerical simulations by the authors, so for simplicity we model data using an isotropic triangular lattice with penetration depth $\lambda_{ab}$. The modeling is performed numerically using straight, rigid vortices with spatial Fourier components given by the London model, which for YBCO is a good approximation in this field and temperature range. The probability distribution obtained from this ideal spatial distribution must then be convoluted with a Gaussian to represent the effects of instrumental resolution. The curve in Fig. 1 gives a value for the average effective penetration depth in the $ab$ plane of $\lambda_{ab} = \sqrt{\lambda_a \lambda_b} = 150(10)$ nm, in reasonable agreement with the estimates of Ref. 20. This is also in fair agreement with values obtained via $\mu$SR on other well-oxygenated YBCO samples at low field and temperature. For example, in Ref. 21 measurements on $YBa_2Cu_3O_{6.955}$ gave $\lambda_{ab} = 140(10)$ nm and in Ref. 22 $\lambda_{ab} = 145.1(3)$ nm was obtained for $YBa_2Cu_3O_{6.95}$, although more recent results by the latter group have recently obtained the somewhat lower value of $\lambda_{ab} = 1155(3)$ nm on samples of the same nominal composition.[23] It is worth noting, however, that as is the case with many techniques which attempt to determine the absolute value of $\lambda$, the values obtained depend to some extent on the details of the model employed. Indeed, as demonstrated by the above examples, values obtained using different models may vary by more than the statistical uncertainty associated with any given fit. Nonetheless, $\mu$SR has been demonstrated to be particularly effective when measuring the *relative* variation of $\lambda$ as a function of changing parameters such as temperature, where the details of the model used do not significantly alter the interpretation.[24,23,22] We adopt this approach in the analysis of the remainder of the data and calculate the anisotropy of the system using only the relative variation of $\langle \Delta B^2 \rangle^{1/2}$ with angle, calculated directly from the measured $\mu$SR spectra. The determination of the anisotropy then follows from Eq. (3). While this approach is still model dependent in the sense that it assumes an anisotropic London model relation between the linewidth and the penetration depth via Eqs. (1) and (3), we make no assumptions concerning the form of the time domain data in order to obtain our frequency spectra. As a further justification of the application of the anisotropic London model, we note that we can use the measured $\mu$SR spectrum to compute the dimensionless quantity $\delta = (B_{\rm peak} - \langle B \rangle)/\langle \Delta B^2 \rangle^{1/2} = -0.60(7)$, where $B_{\rm peak}$, $\langle B \rangle$, and $\langle \Delta B^2 \rangle$ are the mode, mean, and second moment of $p(B)$, respectively. This is in agreement with the value $\delta \approx -0.6$ expected for a triangular lattice in the London limit.[6]

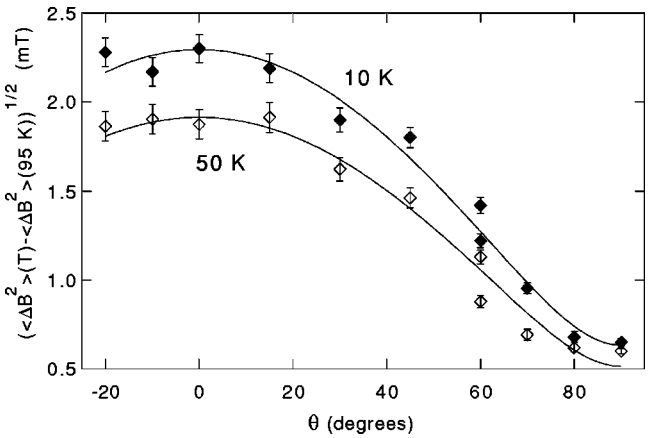


FIG. 3. The variation of $\langle \Delta B^2 \rangle^{1/2}$ with the angle of the trapped field to the $c$ axis, for rotation within the $ac$ plane. The curves show the expected theoretical dependencies for measurements taken at 10 and 50 K, yielding values of the anisotropy parameter $\gamma_{ca} = 3.6(4)$ and 3.7(5), respectively. All measurements were made after cooling the sample from above $T_c$ in an applied field of 20 mT.

Figure 3 shows the angular variation within the $ac$ plane of the rms $\langle \Delta B^2 \rangle^{1/2}(\theta)$, where $\theta$ is the angle of the field to the $c$ axis. Fits of the data to Eq. (3) are also shown, and yield values of $\gamma_{ca} = 3.6(4)$ and 3.7(5) for angular scans at 10 and 50 K, respectively. We note that the measurements at the higher temperature are more difficult due to the smaller linewidth (longer penetration depths), although there is nonetheless good agreement between the values obtained at the two temperatures. Figure 4 shows a graph of $\langle \Delta B^2 \rangle^{1/2}(\vartheta)$ as a function of the angle between the $a$ axis and the field in the $ab$ plane. This yields values for the much smaller in-plane anisotropy $\lambda_{ab}$ of 1.16(2) and 1.15(2) at 10 and 50 K, respectively. This also allows us to derive the third anisotropy ratio $\gamma_{cb} = \gamma_{ab}\gamma_{ca} = 4.5(7)$ at 10 K.

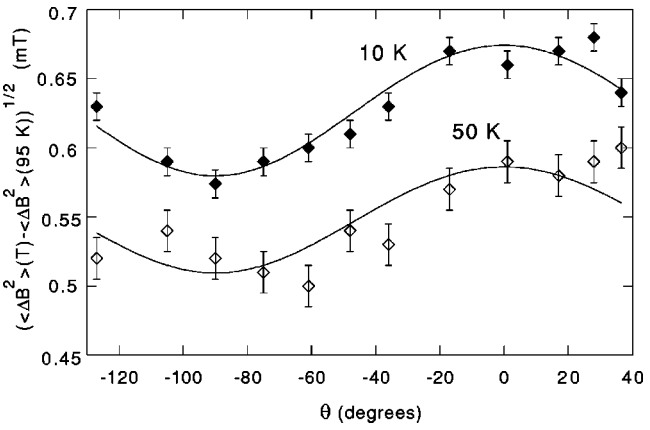


FIG. 4. Variation of $\langle \Delta B^2 \rangle^{1/2}$ with the angle of the field to the $a$ axis, for a rotation within the $ab$ plane. The curves show that YBCO follows the theoretical dependencies for a well-ordered vortex-line lattice at 20 mT ($H > H_{c_1}$) yielding values of $\gamma_{ab} = 1.16(2)$ at 10 K and 1.15(2) at 50 K. All measurements were made after cooling the sample from above $T_c$ in an applied field of 20 mT.

### B. Torque magnetometry

The sample was also characterized using a torque magnetometer. According to calculations based on the three-dimensional anisotropic London model in the mixed state, the reversible torque for rotation between the $c$ axis and the $a$ (or $b$) axis about the third principal axis is given by[25,26]

$$\tau(\theta_{cl})_{\rm rev} = \frac{\phi_o H V}{64\pi\lambda_{ab}^2} \frac{(\gamma_{cl}^2 - 1)\sin 2\theta_{cl}}{\epsilon(\theta_{cl})} \ln\left(\frac{\gamma_{cl}\eta H_{c2}^{\parallel}}{H\epsilon(\theta_{cl})}\right), \quad (4)$$

where $\epsilon(\theta_{cl}) = (\sin^2\theta_{cl} + \gamma_{cl}^2 \cos^2\theta_{cl})^{1/2}$, $\theta_{cl}$ is the angle between the applied field and the $c$ axis, $\gamma_{cl} = \lambda_c/\lambda_l$ ($l$ denotes either $a$ or $b$), $H_{c2}^{\parallel}$ is the upper critical field for the field along the $c$ direction, $\eta$ is a constant of the order of unity and depends on the structure of the flux-line lattice, $\lambda_{ab}$ is the effective in-plane penetration depth, and $V$ is the sample volume. The anisotropy ratios can thus be extracted from the normalized reversible torque signal (see e.g., Refs. 27 and 2). The torque signal $\tau$ was measured on a custom-built magnetometer with a specially constructed sensor to accommodate the same large single crystal used in the muon experiment. Scan angles of over 360° were achieved by step rotation of the cryostat, in which our cantilever and sample were mounted, about a fixed field direction. Torque was measured in the $ca$ and $cb$ planes in a field of 0.66 T and a temperature of 93 K, just below $T_c = 93.5$ K. This point in the phase diagram was chosen to make the torque reversible with negligibly small hysteresis. Figure 5 shows the torque upon rotation around the $a$ axis in the $cb$ plane, as a function of the angle $\theta_{cb}$ between the field and the $c$ axis in the $cb$ plane. In Fig. 5 the line represents the fitting curve using a normalized form of Eq. (4). This gives the anisotropy parameter as $\gamma_{cb} = \lambda_b/\lambda_c = 7.3(5)$. The anisotropy parameter $\gamma_{ca} = \lambda_a/\lambda_c$ was measured by a similar torque measurement around the $b$ axis in the $ca$ plane, which yielded a value of $\gamma_{ca} = 6.6(5)$. The $ab$ anisotropy parameter can then be obtained as $\gamma_{ab} = 1.1(1)$.

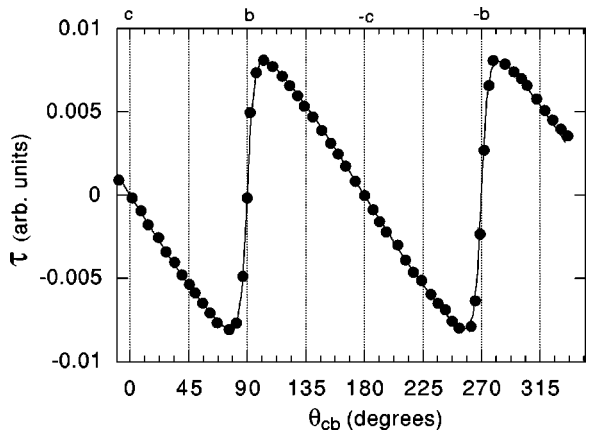


FIG. 5. The torque signal for the untwinned YBCO upon rotating the field of 0.66 T about the $a$ axis at 93 K, just below $T_c$. The line represents a fitting curve based on the London model (see Refs. 25 and 26), yielding an anisotropy $\gamma_{bc} = 7.3(6)$.

## III. DISCUSSION

We begin by comparing our values of the anisotropy constants obtained using $\mu$SR with those obtained by other microscopic techniques, a summary of which is given in Table I. A study on the *same* untwinned YBCO crystal has recently been performed by Johnson *et al.*,[20] using SANS. The in-plane anisotropy $\gamma_{ab}$ could be deduced in that work from the distortion of the diffraction pattern from the vortex lattice observed with the field parallel to the $c$ direction. The resulting value $\gamma_{ab} = 1.18(2)$ is in good agreement with our value of $\gamma_{ab} = 1.16(2)$ from $\mu$SR and $= 1.1(1)$ from torque measurements. In Ref. 20 it was not possible to determine the out-of-plane anisotropies $\gamma_{ca}$ or $\gamma_{cb}$ since at those angles of the field close to the $c$ direction, which were studied, the distortions are not sensitive to these values of the anisotropy. An earlier SANS study on twinned YBCO crystals performed over a wider range of angles[28] estimated the effective mass ratio $M_{ab}/M_c = 20(2)$, leading to $\gamma_{c-ab} = 4.5(6)$, which is not inconsistent with our estimates of $\gamma_{c-ab} = 3.9(6)$ (Table I). It should also be borne in mind that the anisotropy is a function of oxygen doping in YBCO, particularly when comparing the present measurements with earlier $\mu$SR studies[15,19] on a mosaic of *twinned* crystals that estimated $\gamma_{c-ab} \sim 5$. Caution should also be exercised when comparing measurements on twinned and untwinned crystals, since in the former the anisotropic pinning present could lead to subtle aberrations of the apparent anisotropy, since the disorder induced in the lattice could lead to a broadening of the $\mu$SR line shapes.[29] These effects, however, are most pronounced for the field close to the $c$ axis,[30,28] where the contribution to the estimates of the out-of-plane anisotropy are almost negligibly small [c.f. Eq. (3)]. A recent study on the same crystal used in our experiments has been performed using polarized neutrons, where the out-of-plane anisotropy may be estimated from the angular dependence of the components of internal field of the vortex lattice both longitudinal and transverse to the applied field direction.[31,32] Preliminary estimates from that experiment are in reasonable agreement with those presented here.[32]

There is thus overall agreement between $\mu$SR and SANS measurements of the in-plane and out-of-plane anisotropy,

TABLE I. Comparison of the anisotropy ratios obtained from this work with those of previous studies. Since only a limited amount of work is available on untwinned crystals, in order to compare easily the out-of-plane anisotropy with measurements on twinned crystals, values of the average $\gamma_{c-ab}=\sqrt{\gamma_{cb}\gamma_{ca}}$ are also calculated, and denoted $\langle\gamma_{c-ab}\rangle$.

| Anisotropy parameter | $\mu$SR (10 K)[a] | $\mu$SR (50 K)[a] | SANS | Torque (93 K)[a] | Torque[d] |
|---|---|---|---|---|---|
| $\gamma_{ab}$ | 1.16(2) | 1.15(2) | 1.18(2)[b] | 1.1(1) | 1.2(1) |
| $\gamma_{ca}$ | 3.6(4) | 3.7(5) | | 6.6(5) | 7.6(6) |
| $\gamma_{cb}$ | 4.2(5) | 4.3(6) | | 7.3(5) | 9.0(8) |
| $\gamma_{c-ab}$ | $\langle 3.9(6)\rangle$ | $\langle 4.0(8)\rangle$ | $\langle 4.5(6)\rangle$[c] | $\langle 6.9(7)\rangle$ | $\langle 8(1)\rangle$ |

[a]This work.
[b]See Ref. 20.
[c]See Ref. 28.
[d]See Ref. 41.

especially on the same single crystal. It is worth noting that the SANS estimates, which are made from structural distortions of the lattice, reflect the structure that is frozen in at the irreversibility line. The $\mu$SR estimates would be more likely to reflect any temperature dependence of the anisotropy, since although structural distortions contribute to the line shape these are rather subtle effects compared to the influence of the magnitude of the penetration depth. Nonetheless, the $\mu$SR results do not indicate any significant variation of the anisotropy ratios with temperature. It is furthermore worth noting that the agreement between SANS and $\mu$SR data occurs even though the former were measured at very much greater fields (typically $>0.5$ T) than those used in the present study, where nonlocal effects and the influence of the *d* wave order parameter would be expected to play a more significant role.

Our estimates of the in-plane anisotropy $\gamma_{ab}$ are in good agreement with those obtained by other methods documented in the literature which probe the bulk properties. Examples of these are Josephson tunnel junctions,[33] and polarized reflectivity,[34] both of which encompassed our estimates in their lower range of values, and Bitter decoration[3,35] $\gamma_{ab}=1.13$. It has been pointed out by separate authors[3,20,36,28] that any disparity in the the above estimates of $\gamma_{ab}$ for different techniques is primarily a consequence of subtle differences in the oxygen stoichiometry of the different samples. Indeed, it has been suggested that the in-plane anisotropy may be completely dependent upon contributions from the CuO chains due to induced superconductivity from their proximity to the $CuO_2$ planes.[4,37] The lack of any significant discrepancy between measurements reported here and elsewhere in the literature for $\gamma_{ab}$ is thus noteworthy.

For the out-of-plane anisotropy there is less satisfactory agreement between microscopic measurements (SANS and $\mu$SR) and other techniques. In the present study the out-of-plane anisotropy from torque measurements yielded values for $\gamma_{cb}=7.3(5)$ and $\gamma_{ca}=6.6(5)$. These values were extracted using the London model,[25] which has been used previously to interpret the torque measurements of the high $T_c$ superconductors.[27,38–40] The values which we obtain are in reasonable agreement with those recently obtained by Ishida *et al.* on untwinned single crystal YBCO using a similar technique,[41] where fits using Eq. (3) yielded $\gamma_{ca}=7.6(6)$ and $\gamma_{cb}=9.0(8)$, implying $\gamma_{ab}=\gamma_{cb}/\gamma_{ca}=1.18(14)$. However, the average value of the out-of-plane anisotropy in both that study and the present study is significantly larger than that obtained via our microscopic measurements. There are several factors that might be influential in this respect. The equation used to fit the torque data does not take into account the discrete nature of the superconducting planes in high $T_c$ systems.[42] This would not, however, be expected to be significant in YBCO close to optimal doping, since this system is in other respects very well described by an anisotropic London model. Indeed, the same approach[14] is taken when analyzing the neutron and muon data,[15,16,28,20] and the data can be well described in this way. Additional geometric contributions to the anisotropy can arise in torque magnetometry due to the anisotropic ''demagnetizing'' factor, since single crystals are generally platelike. While this would lead to a systematic error in the evaluation of $\gamma_{ca}$ and $\gamma_{cb}$, to a first approximation this would cancel out in estimates of $\gamma_{ab}$ derived from the out-of-plane contributions. This might account for the much closer agreement between all techniques for the in-plane anisotropy compared to the out-of-plane values. It cannot be discounted, however, that the differences between the microscopic and macroscopic approaches might hint at some more subtle consequence of the different way each method probes the anisotropy. SANS and $\mu$SR, for instance, both probe the penetration depths and resulting anisotropy by observation of the vortex lattice, and not via bulk transport currents, albeit in different ways. In addition, torque data generally taken at high temperature in the reversible regime to remove the influence of pinning. $\mu$SR and SANS measurements tend to be made at lower temperatures where the shorter penetration depth leads to wider line shapes and stronger scattering, respectively. Even though performed in the field cooled state, these experiments still probe the irreversible region of the magnetic phase diagram. At present it is not clear, however, how these differences could lead to the observed discrepancy.

In conclusion, we have carried out microscopic and bulk measurements of the in-plane and out-of-plane anisotropies in a large untwinned single crystal of YBCO. The values obtained from $\mu$SR are in good agreement with those obtained via neutron scattering, for both the in-plane and out-of-plane anisotropies. The torque measurements produce values for the out-of-plane anisotropy which are somewhat higher than the $\mu$SR results, although in reasonable agree-

ment with torque measurements by other workers. It is not clear at present whether this discrepancy highlights intrinsic limitations of the different measurement technique, or whether it reflects a more subtle influence of the way the anisotropy is assessed via microscopic and macroscopic techniques.

**ACKNOWLEDGMENTS**

We would like to thank the staff on beamlines M3 at PSI, Zürich and MUSR, ISIS, RAL, for technical support. Financial support from the EPSRC of the UK and the Swiss NSF is gratefully acknowledged.

[1] M.P.A. Fisher, D.S. Fisher, and D.A. Huse, Phys. Rev. B **43**, 130 (1991).
[2] J.C. Martinez, S.H. Brongersma, A. Koshelev, B. Ivlev, P.H. Kes, R.P. Griessen, D.G. de Groot, Z. Tarnawski, and A.A. Menovsky, Phys. Rev. Lett. **69**, 2276 (1992).
[3] D.N. Basov, R. Liang, D.A. Bonn, W.N. Hardy, B. Dabrowski, H. Quijada, D.B. Tanner, J.P. Rice, D.N. Ginsberg, and T. Timusk, Phys. Rev. Lett. **74**, 598 (1995).
[4] J.L. Tallon, C. Bernhard, U. Binninger, A. Hofer, G.V.M. Williams, E.J. Ansaldo, J.I. Budnick, and C. Niedermayer, Phys. Rev. Lett. **74**, 1008 (1995).
[5] A.I. Rykov *et al.*, in *Advances in Superconductivity VIII*, edited by H. Hayakawa and Y. Enomoto (Springer, Tokyo, 1996), p. 341.
[6] C.M. Aegerter and S.L. Lee, Appl. Magn. Reson. **13**, 75 (1997).
[7] S.L. Lee, P. Zimmermann, H. Keller, M. Warden, I.M. Savić, R. Schauwecker, D. Zech, R. Cubitt, E.M. Forgan, P.H. Kes, T.W. Li, A.A. Menovsky, and Z. Tarnawski, Phys. Rev. Lett. **71**, 3862 (1993).
[8] S.L. Lee, M. Warden, H. Keller, J.W. Schneider, D. Zech, P. Zimmermann, R. Cubitt, E.M. Forgan, M.T. Wylie, P.H. Kes, T.W. Li, A.A. Menovsky, and Z. Tarnawski, Phys. Rev. Lett. **75**, 922 (1995).
[9] C.M. Aegerter, S.L. Lee, H. Keller, E.M. Forgan, and S.H. Lloyd, Phys. Rev. B **54**, 15 661 (1996).
[10] S.L. Lee, C.M. Aegerter, H. Keller, M. Willemin, B. Stäuble-Pümpin, E.M. Forgan, S.H. Lloyd, G. Blatter, R. Cubitt, T.W. Li, and P. Kes, Phys. Rev. B **55**, 5666 (1997).
[11] B.D. Rainford, and G.J. Daniell, Hyperfine Interact. **87**, 1129 (1994).
[12] T.M. Riseman and E.M. Forgan, Proceedings of the 8th International Conference on Muon Spin Rotation, Relaxation and Resonance, Les Diableret, Switzerland, 1999 [Physica B (to be published)].
[13] C.M. Aegerter, J. Hofer, I.M. Savic, H. Keller, S.L. Lee, C. Ager, S.H. Lloyd, and E.M. Forgan, Phys. Rev. B **57**, 1253 (1998).
[14] S.L. Thiemann, Z. Radovic, and V.G. Kogan, Phys. Rev. B **39**, 11 406 (1989).
[15] E.M. Forgan, S.L. Lee, S. Sutton, J.S. Abell, S.F.J. Cox, C.A. Scott, H. Keller, B. Pümpin, J. W. Schneider, H. Simmler, P. Zimmermann, and I.M. Savić, Hyperfine Interact. **63**, 71 (1990).
[16] R. Cubitt, E.M. Forgan, M. Warden, S.L. Lee, P. Zimmermann, H. Keller, I.M. Savić, P. Wenk, D. Zech, P.H. Kes, T.W. Li, A.A. Menovsky, and Z. Tarnawski, Physica C **213**, 126 (1993).
[17] A.D. Sidorenko, V.P. Smilga, and V.I. Fesenko, Hyperfine Interact. **63**, 49 (1990).
[18] A.D. Sidorenko, V.P. Smilga, and V.I. Fesenko, Physica C **166**, 167 (1990).
[19] B. Pümpin, H. Keller, W. Kündig, I.M. Savić, J.W. Schneider, H. Simmler, P. Zimmermann, E. Kaldis, S. Rusiecki, C. Rossel, and E.M. Forgan, J. Less-Common Met. **164–165**, 994 (1990).
[20] S.T. Johnson, E.M. Forgan, S.H. Lloyd, C.M. Aegerter, S.L. Lee, R. Cubitt, P.G. Kealey, C. Ager, S. Tajima, A. Rykov, and D. McK. Paul, Phys. Rev. Lett. **29**, 2792 (1999).
[21] P. Zimmermann, H. Keller, S.L. Lee, I.M. Savič, M. Warden, D. Zech, R. Cubitt, E.M. Forgan, E. Kaldis, J. Karpinski, and C. Kruger, Phys. Rev. B **52**, 541 (1995).
[22] J.E. Sonier, R.F. Kiefl, J.H. Brewer, D.A. Bonn, J.F. Carolan, K.H. Chow, P. Dosanjh, W.N. Hardy, R.X. Liang, W.A. Macfarlane, P. Mendels, G.D. Morris, T.M. Riseman, and J.W. Schneider, Phys. Rev. Lett. **72**, 744 (1994).
[23] J.E. Sonier, R.F. Kiefl, J.H. Brewer, D.A. Bonn, S.R. Dunsiger, W.N. Hardy, R.X. Liang, W.A. MacFarlane, T.M. Riseman, D.R. Noakes, and C.E. Stronach, Phys. Rev. B **55**, 11 789 (1997).
[24] J.E. Sonier, Ph.D. thesis, University of British Columbia, 1998.
[25] V.G. Kogan, Phys. Rev. B **38**, 7049 (1988).
[26] L.J. Campbell, M.M. Doria, and V.G. Kogan, Phys. Rev. B **38**, 2439 (1988).
[27] D.E. Farrell, J.P. Rice, and D.M. Ginsberg, Phys. Rev. Lett. **67**, 1165 (1991).
[28] M. Yethiraj, H.A. Mook, G.D. Wignall, R. Cubitt, E.M. Forgan, S.L. Lee, D.M. Paul, and T. Armstrong, Phys. Rev. Lett. **71**, 3019 (1993).
[29] E.H. Brandt, Phys. Rev. B **37**, 2349 (1988).
[30] M. Yethiraj, H.A. Mook, G.D. Wignall, R. Cubitt, E.M. Forgan, D.McK. Paul, and T. Armstrong, Phys. Rev. Lett. **70**, 857 (1993).
[31] E.M. Forgan, P.G. Kealey, T.M. Riseman, S.L. Lee, D.M. Paul, C.M. Aegerter, R. Cubitt, P. Schleger, A. Pautrat, C. Simon, and S.T. Johnson, Physica B **267–268**, 115 (1999).
[32] P.G. Kealey (private communication).
[33] A.G. Sun, S. Han, A.S. Katz, D.A. Gajewski, M.B. Maple, and R.C. Dynes, Phys. Rev. B **52**, R15 731 (1995).
[34] M. Ichioka, N. Hayashi, N. Enomoto, and K. Machida, Phys. Rev. B **53**, 15 316 (1996).
[35] N.L. Wang, S. Tajima, A.I. Rykov, and K. Tomimoto, Phys. Rev. B **57**, 11 081 (1998).
[36] B. Janossy, D. Prost, S. Pekker, and L. Fruchter, Physica (Amsterdam) **181C**, 51 (1991).
[37] V.Z. Kresin, and S.A. Wolf, Phys. Rev. B **46**, 6458 (1992).
[38] K. Okuda, S. Kawamata, S. Noguchi, N. Itoh, and K. Kadowaki, J. Phys. Soc. Jpn. **60**, 3226 (1991).
[39] D. Zech, J. Hofer, H. Keller, C. Rossel, P. Bauer, and J. Karpinski, Phys. Rev. B **53**, R6026 (1996).
[40] D. Zech, C. Rossel, L. Lesne, H. Keller, S.L. Lee, and J. Karpinski, Phys. Rev. B **54**, 12 535 (1996).
[41] T. Ishida, K. Okuda, H. Asaoka, Y. Kazumata, K. Noda, and H. Takei, Phys. Rev. B **56**, 11 897 (1997).
[42] L.N. Bulaevskii, Phys. Rev. B **44**, 910 (1991).